On-time EM measurements: UTEM system developments

Lamontagne Y.*[1], Langridge R.[1]

1. Lamontagne Geophysics Ltd., Kingston Ontario, Canada

ABSTRACT

The recent evolution of the UTEM system (UTEM 5) aimed to perform essentially the same geophysical measurements as UTEM 1 with a much greater precision, at frequencies that are up to 100 times lower and measuring multiple components and multiple transmitters at once. The rationale of the system is to provide uniform exploration search over the wide range of conductor conductivity, size and depth encountered in exploration. One part of the recent hardware developments has been the development of more efficient high power high voltage digitally controlled transmitters. The other part has been the joint development of a low noise low frequency 3-axis sensor and a receiver which uses enhanced noise reduction techniques and is capable of simultaneous multiple transmitter data acquisition and of live data reduction for in-field monitoring purposes. The depth capability of the new surface UTEM system is more than two times greater than that of the system it replaces. Its relative advantage is greater yet for low frequency measurements.

INTRODUCTION

UTEM is a large loop time-domain EM system that measures during the on-time. "Time-domain" measurements originate in radar and reflectometer instruments which record the signal after a transmitted pulse to detect reflections. This measurement method was first introduced to geophysical EM exploration in the sixties with the Barringer/Questor Input airborne EM system. Measurements are made after transmitter turn-off to separate the secondary field from the primary field while getting geophysical information over a range of frequency.

The idea behind an "on-time" time-domain system is to keep some of the advantages of conventional transient measurements such as efficiently measuring over a range of frequencies while being able to obtain the equivalent of the frequency domain in-phase response. The first system was developed in 1971-1972 as a doctoral thesis project at the University of Toronto from which it got its name, UTEM (Lamontagne, 1975). The system has since evolved towards a wider bandwidth at the low frequency end, to higher precision, and to include multi-component sensors for both surface and down-hole measurements.

The system philosophy has remained the same which is to provide as much as possible a uniform coverage over a wide range of time decays and also deep uniform coverage in space over a large range of distances or depths through the use of large transmitter loops. The evolution since 1972 has been one of degree: going from 256:1 time range to 4096:1 or more, from 2-3% precision to <0.1%, from 600 m distance from the loop to more than 2000 m, from 30 Hz minimum frequency down to 0.25 Hz, from single component/single transmitter to 3-axis multiple transmitters data acquisition, from surface

Table 1

Year	Version	EM fields	Notes
1972	UTEM 1	dB/dt	thesis project
1976	UTEM 2	dB/dt, E	U of T/industry consortium digital recording
1981	UTEM 3	B (FB coil) E	PE/DC Cominco funding
1983	BHUTEM 3 2200m cable	B axial	borehole UTEM fibre optic link
1988	ISR CE	E	ISR capacitive electrodes
1989	BHUTEM 3H 3300m cable	B axial	deep hole BH UTEM deep fibre optic link
1990	UTEM 3E	B, E	level 4 PE/DC, 2Hz master/slave TX
1996	BHUTEM 4 UTEM 4 RX	3-axis B	3-axis FB BH sensor, U4RX Inco funding
2002	UTEM 4 TX		High power digital WF TX Falconbridge/Cogema funding
			Last 10 years
2010	LF ISR CE	E	Low frequency capacitive electrodes ISR imaging
2011	UTEM 5S	3-axis B	UTEM 5 3-axis surface FB UTEM 5 receiver 3-TX stacking
2013	UTEM 5 ISR	3-dipole E	UTEM 5 3-dipole E field, ISR
2014	UTEM 5M TX		UTEM 5 transmitter M power
2017	UTEM 5H TX		UTEM 5 transmitter H power

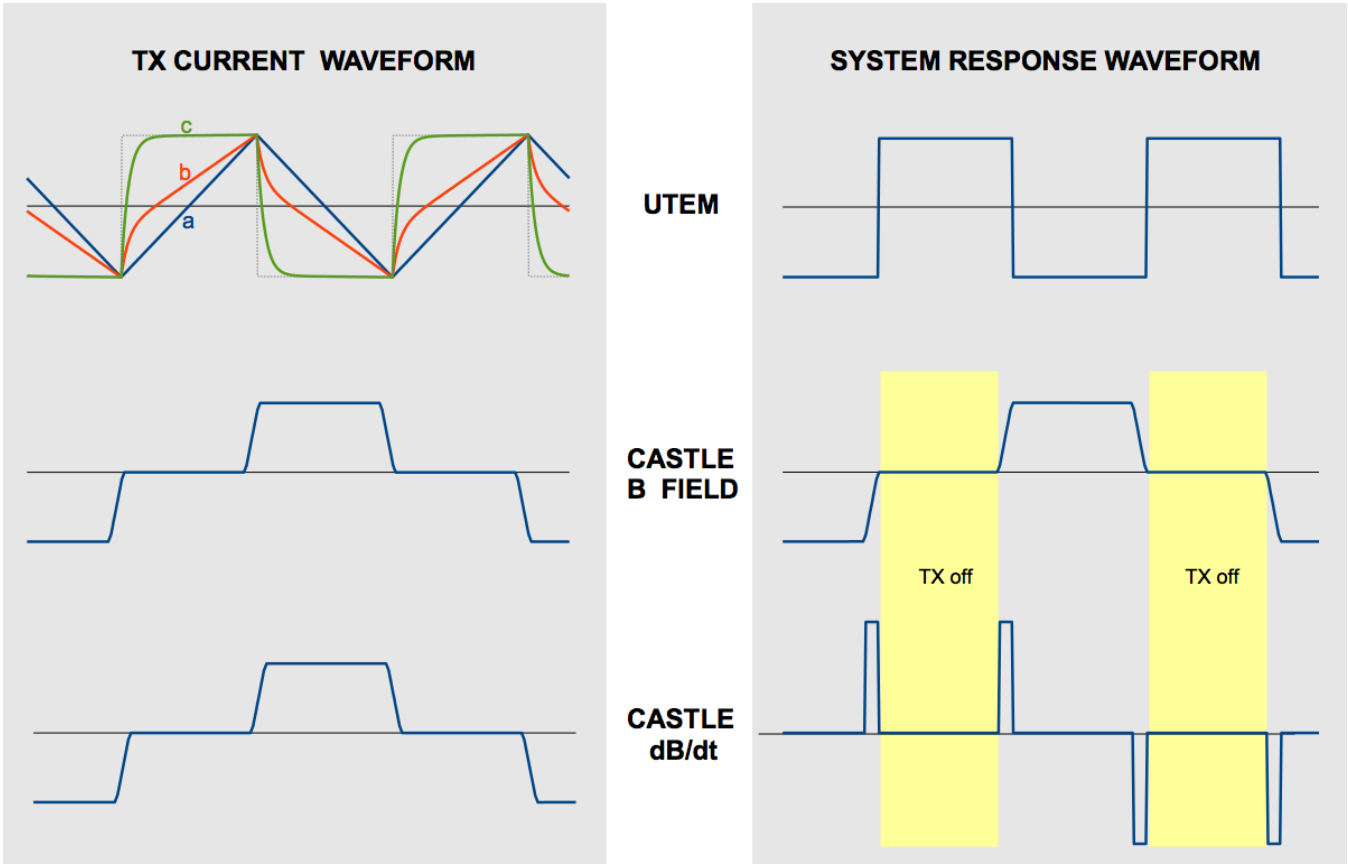

Figure 1: *The evolution of the UTEM transmitter current waveforms from* ***(a)*** *a ramp waveform (UTEM 1 and UTEM 2) to (b****)*** *moderate levels of PE (UTEM 3) and then* ***(c)*** *to more extreme PE possible with UTEM 4 and 5 high slew rate transmitters. The PE waveforms are shown with much exaggerated rise time length. The UTEM system response for both magnetic and electric fileds has always remained a square wave. We define the system response as the primary field waveform seen by the receiver channel sampler. For comparison the typical castle current waveform used in fixed loop off-time measurements is shown with the corresponding system responses waveforms obtained in B field measurements and in dB/dt measurements.*

dB/dt only to surface B/E field and downhole B field. Table 1 shows the main development steps in UTEM instrumentation before and after the 2007-2017 decade. This article documents some of the developments over the last decade but also includes an important transmitter advance from the previous decade not described in the 2007 DMEC paper which was centred on borehole EM methods (Lamontagne, 2007).

WAVEFORMS AND SYSTEM RESPONSES

Measuring the step response

For EM measurements, the step response has very desirable properties in that the **inductive limit** (IL) and **resistive limit** are easily measured and that the wideband response can be measured using a dynamic range which is similar to that of the measured primary field strength. The square wave is the most effective periodic approximation of the step response that can be used in practice. A square wave of unit amplitude is made of a superposition of steps two units high of alternating polarity every half-cycle.

Inductive limit

The most important of these measures is the IL. It is the limit of the response at high frequency which for a conductor in free space depends only on the geometry of the conductor irrespective of its conductivity i.e. conductor shape, size, and position relative to the transmitter and survey line. If the inductive limit response is normalized to the primary field at each station, its amplitude depends mainly on the ratio of the depth to size of the conductor and on the coupling angle of the primary field.

For the **step response** the limit of the response at early time is the same as the IL (Laplace's initial value theorem). The properties of the IL strictly valid for free space conductors also applies for a very high contrast conductor if the early response is estimated after the background response has subsided. For a **square wave** the initial response ranges from two times the inductive limit for

responses with decay times shorter than the half cycle to one time the inductive limit for extremely much longer decay times. In the general case the inductive limit can be estimated as the half sum of the early time limit and the response at the end of the half cycle.

System responses

UTEM is thus defined as a system with a square wave system response meaning that in the absence of any earth response the primary field waveform sampled by the receiver is a square wave with channels of constant amplitude in each half cycle.

This is explained in **Figure 1**. The actual transmitter current waveforms used in various UTEM versions are compared to those of off-time castle waveform systems. In the days of UTEM 1 and also with UTEM 2 (West et al., 1984) the square wave response was accomplished by transmitting a triangular waveform (a) and sensing the dB/dt field which was sampled as is (Fig **1,** curve a). With UTEM 3, B field feedback sensors started to be used and pre-emphasis/deconvolution (PE/DC) was introduced to improve the signal to noise of the sampled signal (Macnae et al., 1984). The transmitted waveform was put through a linear filter to emphasize the high frequency part before being transmitted (curve b) and a deconvolution filter applied to the B field so the primary signal waveform sampled by the receiver remained a square wave.

The degree of PE/DC initially used in UTEM 3 (level 1) was relatively mild (3.5:1 high frequency pre-emphasis) being limited by the slew rate limit of the transmitter. It still led to substantial improvement in repeatability on all channels. As base frequencies were lowered and the UTEM 3 transmitter voltage slew rate capability was increased the level of PE/DC was increased in four levels up to a maximum pre-emphasis of 74:1 at some low base frequencies in UTEM 3E.

With the UTEM 4 transmitter output power was increased by a factor of 5 and the slew rate limitation was mostly removed so the PE/DC filters could be tailored to individual transmitter loops, ambient noise spectrum, and sensor sensitivity to optimize the post-stack precision relative to the primary field. So with the UTEM 4 transmitter the current waveform in many applications looked generally like a square wave (Fig. **1**, curve c) except in the detail of the rise time at the polarity transitions. The frequency response of the deconvolution filters in these cases are then almost flat except above 100 Hz.

For comparison the current waveform and system response waveforms of off-time surface EM system are shown. In **Figures 1D** and **1E** the typical current waveforms of off-time system and the corresponding systems responses are shown for B field and dB/dt systems respectively.

For the UTEM system, whether the sensors actually measure the dB/dt or the B field, the system response of the system from a geophysical response point of view has remained a square wave response. This is also true for E field measurement for which the raw primary signal has the same waveform as the dB/dt field. In all cases the respective deconvolution filter applied is designed so the resulting primary signal is a square wave. From a signal level point of view the UTEM measurements with UTEM 4 and UTEM 5 are now very similar to B field measurements whereas with UTEM 1 they were true dB/dt measurements. All measure the same square wave response.

Decay time sensitivity

Measuring in the "on-time" involves added complexity in the instrumentation and in the field procedure. The survey geometry must be known precisely to reduce errors in the primary field reduction. The transmitter current waveform must be regulated continuously and the system must behave linearly throughout. The well known advantage of on-time measurements in general terms is that they can detect highly conductive bodies even those with no decay within the range of sampling times.

The decay time T of the inductive response of a finite conductor is expressed in terms of the conductivity of the body σ and its two smallest dimensions the thickness E and width W by the formula:

$$T = K\sigma\mu EW \qquad (1)$$

where K is roughly 0.1 for most shapes and μ the magnetic permeability is nominally $4\pi \times 10^{-7}$.

The free-decaying response of finite conductors behaves exponentially at late time so responses with exponential decay are used to compare the effectiveness of different time-domain EM systems to conductors of varying quality. **Figure 2** shows the sensitivity of system responses to five exponential decays of lengths varying from 1/16 to 16 times S which is the half-cycle of the UTEM waveform or the quarter cycle of the castle waveform. For an equal sampling range in the off-time compared to that of a square wave system in the on-time, the base frequency of the castle waveform must be slightly less than half that of the square wave. The number of sets of channels stacked per unit time will be half that of the square wave system.

For UTEM (A) the initial response amplitude varies by a factor of two over the whole range of decay times from an amplitude which is twice the IL for short decays to a non-zero amplitude equal to the IL at the high end i.e. for infinitely long decays. It is evident that for the castle waveform the strongest secondary field response whether B field (B) or dB/dt (D) occurs during the "on-time of the transmitter including the ramp time. Effectively measuring in the off-ime is less efficient from a signal recovery point of view. On the other hand it is popular because (1) it is possible to use a simple brute force transmitter without precise current waveform regulation and (2) because a nominal survey grid can be used since the primary field does not need to be subtracted to obtain the secondary field. Both of these differences result in a lower survey cost.

For B field off-time measurements (**Figure 2B**), the response is relatively smaller for decay times shorter than the ramp time of the castle waveform. As the decay time increases the peak response reaches a maximum slightly less than the inductive limit for a decay time shorter than S and then decreases vanishingly as

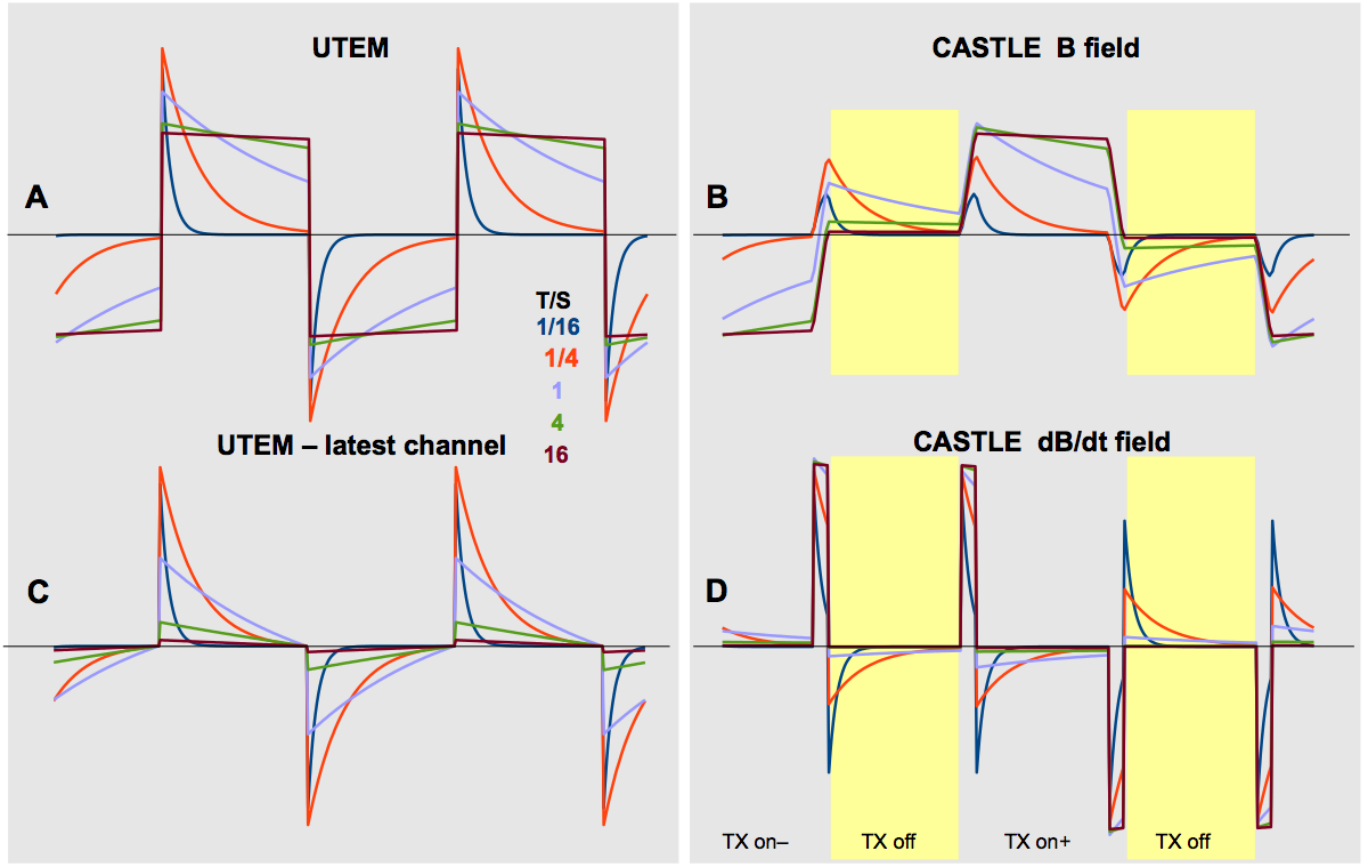

Figure 2: *Comparison of five exponential decay responses for the on-time square wave system response (UTEM) and the "castle" waveform used by off-time systems. The UTEM and B field castle response are at the same scale assuming the same peak-to-peak primary field excitation. The time constants of the responses range from S/16 to 16 S where S is half the UTEM period or a quarter the castle waveform period. The yellow bands indicate the ranges of off-time in the castle waveform, which is S minus the ramp time. For very long decay times the UTEM response is un-decaying with amplitude limit which is half the amplitude of a short decay response. In the off-time of the castle waveform the response vanishes for very long decay times but it does so at lower decay times for the dB/dt field.*

the decay time T becomes much greater than S. For the largest T/S of 16 shown the maximum response in the off time is less than 3% of the inductive limit response.

The **late channel corrected** UTEM response shown in **Figure 2C** has the same initial amplitude as the uncorrected response in A for short decay time but decreases for very decay times longer than ≈S/2 as do the off-time B measurements. For very long decay times the late time corrected UTEM response (**Figure 2C**) tends to a limit which is twice that of the off-time B field of **Figure 2B**. The primary field reduced late time channel which at the high is equal to the IL is usually plotted separately.

Castle dB/dt measurements cannot be easily compared to B field measurements being measured in different units. Compared to dB/dt ramp current (UTEM 1 and 2) systems, it can be shown that a castle waveform dB/dt system has the highest off-time response for very short ramp off times and in these cases it has a responses larger than the dB/dt UTEM 1 (and UTEM 2) system for T < S/8.

OBJECTIVES OF THE DEVELOPMENTS

The design objective of the UTEM system has remained to provide as much as possible a tool with uniform coverage in mineral exploration. This means uniform coverage over induction parameters which in the time-domain are decay times and also as much as possible uniform coverage in depth or lateral position.

Towards this objective, developments on multiple fronts have resulted in a widening of the range of the UTEM equipment to lower base frequencies and also in an increase in the depth /distance of investigation. Four sub-systems were affected:

1) UTEM 5 transmitter system
2) UTEM 5 surface EM sensor
3) UTEM 5 receiver system
4) UTEM 5 ISR capacitive electrode system

There were also developments in data processing and modelling tools aimed at making the data easier to analyze and interpret in terms of exploration models:

1) Web based tools for data reduction and plotting
2) MultiLoop and MGEM modelling software
3) ISR imaging

This article will concentrate on the recent transmitter, surface sensor and receiver developments.

UTEM DEVELOPMENTS

Transmitter developments

The major advance in UTEM transmitter technology took place in 2002-2003 with the introduction of the UTEM 4 transmitter first as a prototype and then as production transmitters. The recent advance in 2015-2017 is more qualitative consisting of increases in efficiency, output level, and waveform precision. In common with the UTEM 3 transmitters, the UTEM 3 and 4 systems are transmitters that continuously regulates the output current and incorporates a differential output that doubles the output voltage swing across the loop.

With the UTEM 3 transmitter this was achieved using a high voltage, high power linear amplifier operating in a feedback loop to regulate the output current (**Figure 3**). An output voltage tracking switch-mode pre-regulator (not shown) was used to reduce power consumption. The pre-emphasis filter was applied in the waveform generator circuit as an analogue active filter on the ramp reference waveform prior to transmission. Depending on the receiver model, the deconvolution filter was either an active analogue filter acting on the analogue signal or a digital filter applied on a time series representation.

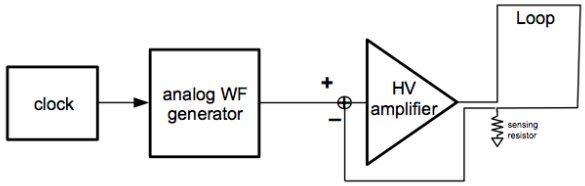

Figure 3: *Block diagram of a one-sided transmitter showing principle of a current regulating transmitter using a Class A high voltage linear amplifier output stage in negative feedback. The actual UTEM 3 transmitter has differential output.*

The goal of the next transmitter generation (2002-2003, UTEM 4) was to synthesize the pre-emphasized waveform digitally and to achieve the current regulation using a switch mode system with higher output level and in particular much higher voltage slew rate than the linear UTEM 3 systems. The system is entirely digital (**Figure 4**) except for current sensing. All connections between the control unit and the power mainframe use fibre optic transmission to avoid interference from the high frequency switching. This design was implemented in a high power configuration only (**Figure 5**) suitable for surveys in areas accessible by road. For continuous full power use, the system (requiring an 11 kW generator) has a peak-to-peak voltage swing capability of 1050V. The system is tailored for large loops of light gauge wire typically of 1500m size providing a dipole moment of 20 million A.m2. At each half-period transition thus there is a dipole moment change of 40 million A.m2.

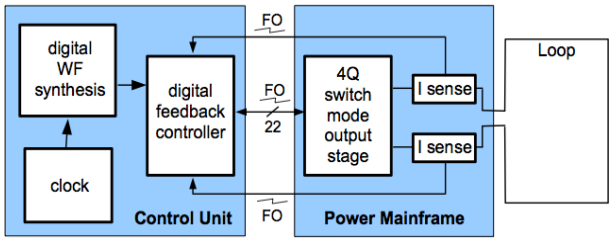

Figure 4: *Simplified block diagram of UTEM 4 transmitter showing digital waveform current regulator and separate fibre optic isolated power mainframe unit.*

Figure 5: *UTEM 4 transmitter setup. The control unit on the left is connected to the 1.4m long power mainframe unit by a cable of multiple optical fibres. The 11kW power generator is off the photograph.*

Figure 6: The *UTEM 5 transmitter prototype. The control unit on the left is >3 m away from the power mainframe during operation. A 30cm ruler shows the scale*

The UTEM 5 transmitter (**Figure 6**) is a more compact system with output voltage swing increased by 20% and maximum current levels increased by 15%. The efficiency of the system is much improved so cooling can be achieved in a smaller shape factor. The system requires 30% less input power at full output. Or it can be used at reduced power with lighter motor generators for portable operation.

The new system has a simpler configuration as reflected in the block diagram (**Figure 4**). Not shown on **Figure 4** is the higher efficiency switch-mode power supply circuitry operating at MHz frequencies. The output stage uses a regenerative design to implement a 4-quadrant voltage/current operation more efficiently. This system recovers the energy stored inductively in the loop in each half-cycle of the waveform while regulating the current.

The critical parts of the system for accurate current regulation are the two current sensing circuits which use oversampling A/D converters operating at 40 Mbps in the UTEM 4 system and at 120 Mbps in the new system. The aim is to improve the waveform fidelity to 0.01% level in the UTEM 5 TX from an estimated 0.03% in the UTEM 4 TX. This is a critical characteristic of the system for detecting very small decaying responses in the presence of the primary field.

UTEM 5 sensor development

Another notable advance is the development of the UTEM 5S sensor which is a 3-axis field feedback coil sensor. In a field feedback induction sensor (**Figure 7**) an induction sensor is used as a null detector in a sensor that cancels out the time varying field within a volume enclosed by feedback windings. In such a coil the H field needed to cancel the field is the actual measurement. So strictly speaking it is an H field sensor. One advantage is that the H field measurement is not affected by any frequency response or temperature coefficient effects due to the properties of the magnetic core or of the sensing coils within the feedback bandwidth.

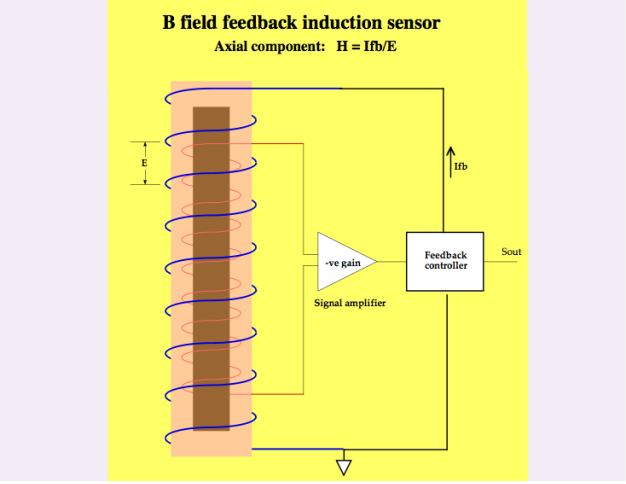

Figure 7: *Sketch showing the principle of a B field feedback induction sensor for a single component. The output of the sensor is actually a measure of the H field.*

In the new UTEM 5 surface sensor as in the BHUTEM 4 the sensor has three axes meaning there are three orthogonal sensors centred on the same point. The self-calibrating totally digital feedback controller (**Figure 8**) has adjustable closed loop compensation and adaptive DC bucking. It uses a low latency oversampling A/D converter at the input and a D/A converter generating the feedback currents. The front end A/D data rate is 224 Mbps.

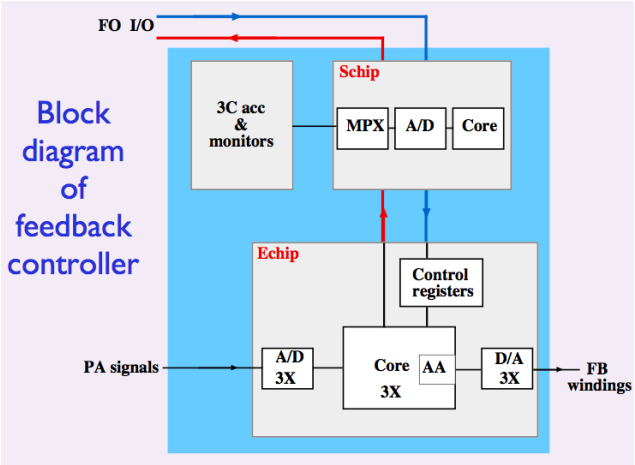

Figure 8: *Feedback controller of the UTEM5 surface sensor. There are three input signals to the Echip section from the pre-amplifiers and three pairs of feedback windings. The Schip controls and encodes the accelerometer, temperature, and voltage monitors. All interconnections between modules are done using fibre optic links.*

As is also done in the UTEM 4 down-hole sensor the output EM data are actually acquired within the controller by averaging and sampling the digital feedback signal that is a measure of the H field. The output of the coil is a pulse code modulated optical signal of all three components plus ancillary data every 10 µs. To avoid stray coupling of the controller circuitry and of the circuitry associated with the orientation tools, all interconnections between modules and to the receiver are done with optical signals and the electronics are shielded within the magnetic core of the coil sensors. **Figure 9** shows the sensor with the fibre optic receiver cable connected to it. The axis of the sensor must be sighted along the survey line but the receiver can be anywhere at some distance from the sensor. **Figure 10** shows the usual field configuration of the sensor and receiver along a test line.

Figure 11 shows the wideband noise spectrum of the sensor calculated from three time series from measurements acquired in a magnetically shielded enclosure. The sensitivity is better than 1 pT/sqrt(Hz) above 0.3 Hz on all components with a noise floor ranging from below 0.01 to 0.03 pT/sqrt(Hz) on the axial (in-line) and transverse components respectively. The stacked data precision is also dependent on the noise rejection techniques used in the receiver.

Figure 9: *UTEM 5 sensor with field tripod legs attached. The fibre optic cable (red) is 9 m long and connects to the UTEM 5 receiver.*

Figure 10: *UTEM 5 surface sensor and receiver layout along a test line. To minimize noise due to operator motion the two instruments are set >8m apart.*

UTEM 5 receiver development

As for the UTEM 4 receiver, the UTEM 5 receiver is totally digital from input signal to output data transfer. For both borehole (BHUTEM 4) and surface (UTEM 5S) sensors the connection to the receiver is done through a fibre optic cable transmitting a pulse code modulated signal.

The front end of the receiver is a decoder that is an extension of the circuitry inside the sensors. This decoder expands the pulse code modulated signals into 3-axis EM data, 3-axis accelerometer data for orientation and other ancillary data such as temperature, battery levels and overload monitors.

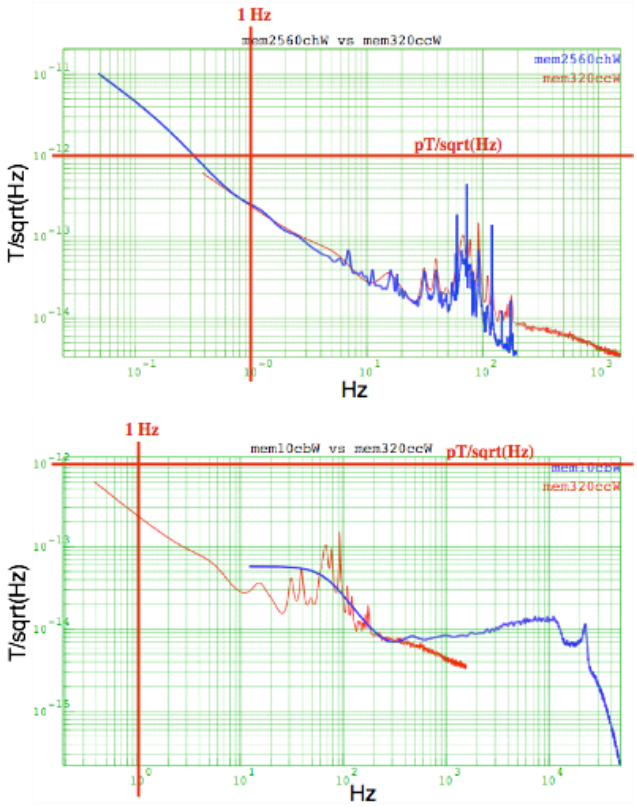

Figure 11: *Wideband spectrum of the UTEM 5 sensor over two frequency ranges measured in a shielded enclosure. Shielding was imperfect allowing power line noise up to one decade above the 10^{-14} noise floor.*

Table 2

Processing of data records	Extra processing for monitoring in the field
decoding	*tensor calibration*
final decimation	*hole/line geometry*
DC compensation	*orientation*
deconvolution filtering	*primary field normalization*
channel sampling	*secondary field reduction*
stacking	*stack progress*
overload level monitoring	*signal level warnings and overloads*
processing of ancillary measurements	*real time channel or profile display*
flash memory recording	*error trace warnings*

The decoded data have 32-bit resolution. The bit level processing is done by digital circuitry whereas the final stage of the decoding is done by signal processors. There is different low level decoding for the BH UTEM 4 data but the same internal numerical representation and code is used in the geophysical data acquisition. After full decoding the receiver signal processor receives three 64-bit words of EM data and a 64-bit time stamp for every 10 µs time interval. It also receives data from the orientation tools (3-axis accelerometers and also 3-axis magnetometers for the borehole sensor) and other ancillary measurements at a lower data rate.

There are two sequences of operations applied to the input data in the receiver: one for data acquisition/recording purposes and the other for field monitoring as listed in Table 2.

There are three main advances in the UTEM 5 receiver:

(1) A data decimation method which together with the A/D and D/A encoding in the U5S sensor gives a code with 32-bit resolution and extremely linear representation of the measured field.
(2) An adaptive DC bucking compensation method that operates with no low frequency roll-off
(3) An enhanced stacking method applied to respective channel data at each half-cycle made of three cascaded processes: a binomial pre-stack, a boxcar average over sub-stacks optimal for frequency interleaving, and an average of sub-stacks.

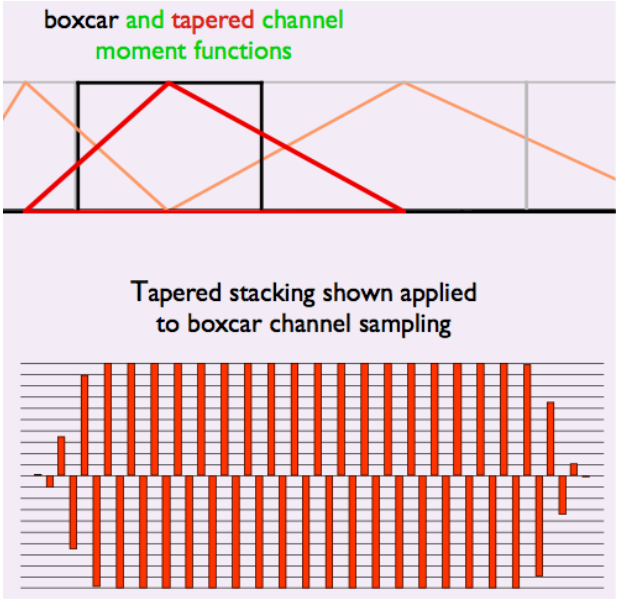

Figure 12: *The sketch at the top compares the sampling functions for boxcar and tapered (bilinear) channels. The bottom sketch shows the combined tapered weighting effect of a cascaded binomial and boxcar stack.*

The combined effect of pre-stack and boxcar stacking is a stack with tapered weights (tapered stack) which is a generalization of the linear tapered stack used in the UTEM 4 receiver.. Other features carried over from the UTEM 4 receiver and applied more effectively with higher resolution data include tapered weight channel sampling scheme (**Figure 12**) which is particularly effective at rejecting non-harmonic power line noise in the wider late channels.

Figure 12 also illustrates the combined data sampling function of a short tapered stack applied boxcar channel sampling. Tapered stacking is very effective at rejecting low frequency noise in the measured field and also at reducing the effect of cultural noise located in spectral bands between the UTEM signal harmonics. This is particularly important when doing EM measurements around mining operations with sources of low frequency noise such as primary crushers, long conveyor belts, etc. Tapered stacking is also effective in the presence of natural low frequency noise such as micropulsation noise.

Figure 13: *A UTEM 5 receiver mounted on its packframe with tripod legs connected to the UTEM 5 sensor in hilly terrain.*

The receiver (**Figure 13**) can sample each component with three channel schemes. So the receiver can at once stack up to nine sets of channels, three sets per component. The three sampling schemes usually measure the respective response of three transmitters running at interleaved base frequencies for which the sub-stack stacking is optimized. The receiver automates the

selection of up to three interleaved transmitter frequencies taking also into account one given power-line frequency. Among other receiver functions there is one for oscilloscope viewing of the signals with automatic anti-aliasing and another for the acquisition of time series of the 3-axis data at a sampling rate of up to 100 kHz.

Since the UTEM system is aimed at performing contract geophysical surveys it was designed so data can be monitored in the field to detail anomalies as required. It is also more cost effective to detect and repeat suspected erratic readings at survey time rather than having to setup the transmitters again to repeat some measurements at a later date. Data can be monitored after orientation to a selectable orthogonal axis system that can be aligned to the traverse lines or in geographical orientations. The data can be monitored with absolute or primary field normalization, with total, secondary late channel reduction. The display can show channel decay or profile plots.

For this purpose the complete survey geometry can be uploaded to the receiver or a nominal geometry entered. The primary field reduction makes it possible to detect and detail suspected undecaying "channel 0" anomalies right at survey time. The frequency of any transmitter and corresponding receiver sampling scheme can be changed at survey time if needed to detail an anomaly.

The receiver records in flash memory the raw data rather than the reduced data so the geometry and calibration data can be refined before final reporting. The data records include all measurements conditions including operator tags, signal monitor logs and settings from the sensor and receiver.

Towards femtotesla precision

The aim of the last developments was to improve the precision EM measurements by more than an order of magnitude at the same base frequency and to push the minimum base frequency down to well below 1Hz. This required major instrumentation improvements as described above and also changes in many aspects of the field procedure.

As far as the instrumentation is concerned its performance was tested by doing repeat data stacks in a quiet shielded environment. In low noise conditions the stacked data precision is mainly dependent on the base frequency and stacking time. Table 3 shows the RMS errors observed in such tests for the same 180s stack lengths at frequencies of 4Hz to 0.22Hz on the last three channels. The percentage error is calculated for measurements outside a 1500 m square loop with 9 A current. So at 1Hz, the RMS error per ampere would be 5fT/A and a precision better than 0.1% would be expected at a 1500m distance from the transmitter. In normal field survey practice multiple stacks (2x or 3x) of 60s to 100s are recorded which would match the stacking time of the tests. The data scatter in actual field measurements even in good conditions is expected to be greater than that in Table 3 due to the presence of ambient noise. In quiet survey areas it is found to typically approach this precision to within ≈40% on most stations.

Table 3

	RMS error	% at 750m	% at 1500m
4Hz	20 fT	0.006%	0.026%
1Hz	45 fT	0.014%	0.056%
0.5Hz	90 fT	0.028%	0.11%
0.22Hz	0.3 pT	0.091%	0.375%

Figure 14 shows an example of multiple "zero" readings recorded at the end of a survey day near Sudbury. This example also shows the dramatic noise effect of road traffic clearly visible within 250m. In cases like this it is suspected that the noise is due mainly to ground vibration rather than the magnetic field effect. The electrical noise from cultural sources such as power-line, protected pipelines or other geophysical systems can be rejected to a high level by the sampling and stacking techniques of the system. Measurements can normally be made within 75m of major power-lines and data precision is mostly unaffected at a distance of 200 m.

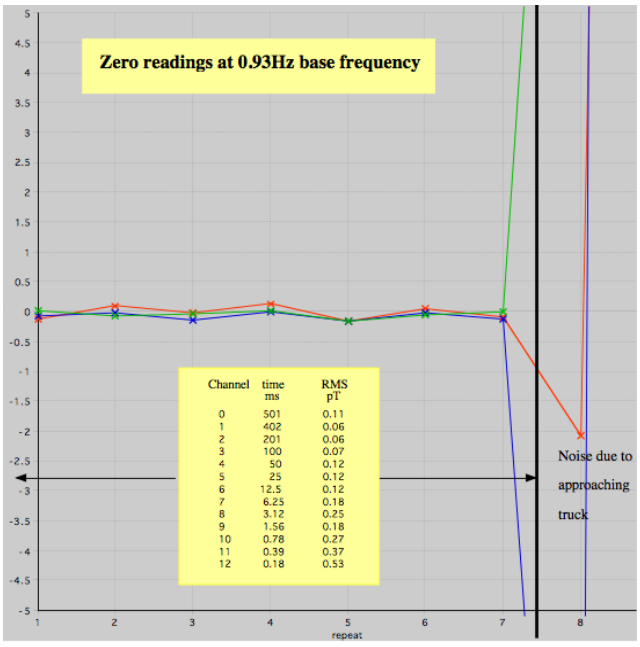

Figure 14: *Repeat 120s stacks for 3 last channels of vertical B field data with no transmitter signal at 0.93 Hz. A survey truck comes within 250m of the sensor during the 8th stack. The RMS error was calculated for all channels using the 8 unaffected stacks.*

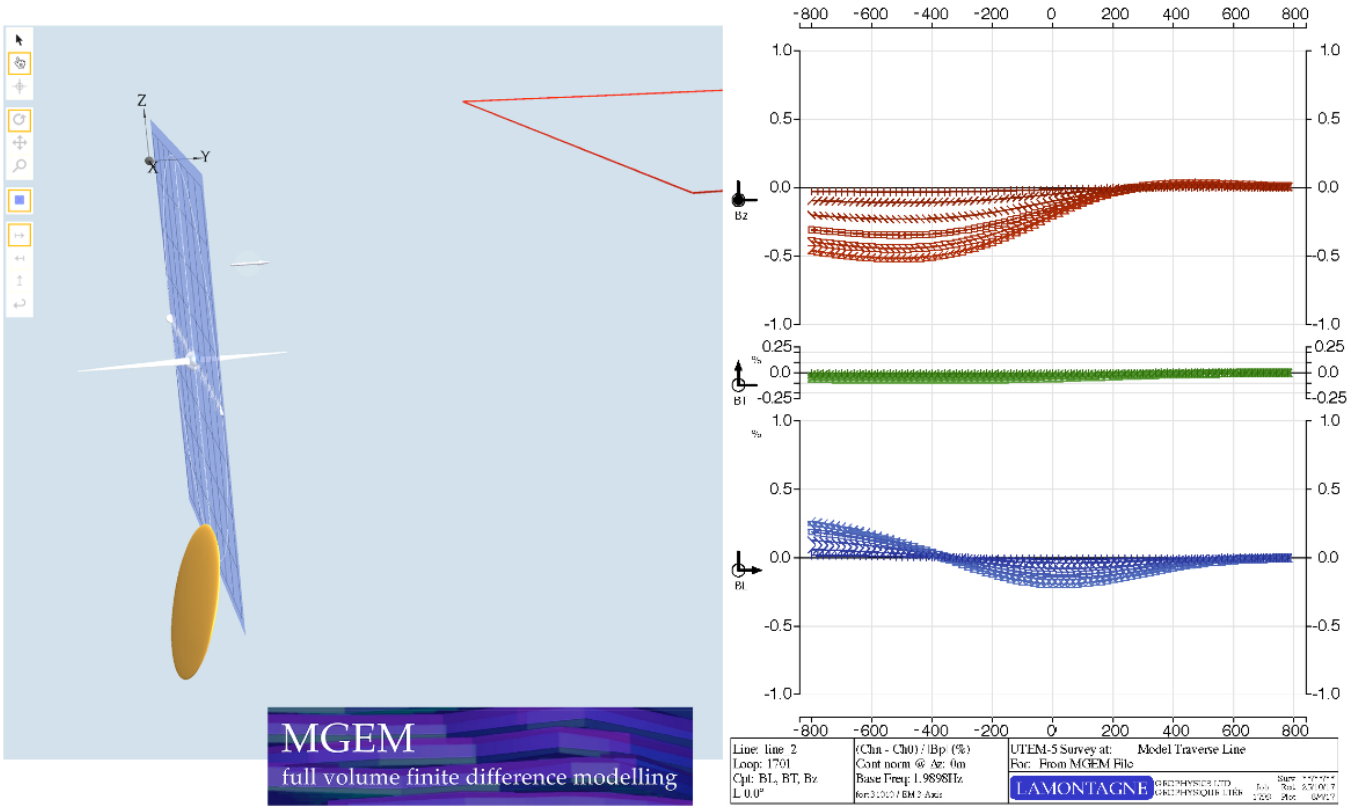

Figure 15: *Test blind conductor used in detectability test and the late channel reduced UTEM response obtained at 2 Hz base frequency in a 20,000 Ωm half-space. The test target is a 100 S/m ellipsoid 40m by 440m by 290m at 750m depth-to-top and located 675m from loop front (under station 125).*

High precision EM field procedures

It was found that in doing high precision EM measurements a very difficult aspect is to avoid outlier measurements that have much higher scatter. It is difficult because even then the absolute errors are so small that they are difficult to detect in the field even though they are obvious after the final data reduction. Including full continuous data reduction in the receiver during staking is helpful in this respect. It helps catch many of these errors because of abnormal settling of the reduced data can be noticed during stack progress with the same reduction and scaling as in the final plots. The main cause of outlier readings is slight sensor rotation during measurements due to its settling in soft ground but it can be also the effect of wind either directly or indirectly by minute motion in the roots of trees near the sensor. Any bush twig or leaf brushing on the sensor has an effect. Station offsets along and across the line can be used to avoid troublesome station setup locations while being taken into account in the geometry of the data recorded and observed in the receiver display.

Survey progress can be impeded within some distance of roads as measurements need to be interrupted at the approach of heavy trucks or machinery. Crew activity in the vicinity of the sensor during measurements also increases the noise level and must be kept to a minimum. It was found necessary to lengthen the coil cable so the receiver operator keeps at least 8 m away from the sensor during measurements and to change the field procedure so the sensor operator is immobile and at least 10m away from the sensor. To avoid wind noise the use of a wind shield has become standard practice in open areas.

To reduce greatly primary field waveform distortions due to capacitive current leakage., the transmitter loop wire was changed to a wire type using insulation with low dielectric constant. This is particularly beneficial in melting snow conditions keeping the squareness of the primary field waveform generally to within 0.02%.

IMPLICATIONS FOR MINERAL EXPLORATION

Although EM methods in general and UTEM in particular can be used for other purposes such as engineering or geological studies, mineral exploration remains the main application of EM induction tools.

The developments of the UTEM instrumentation and software in the last decade were aimed at doing measurements at lower frequency and with greater precision. The main objective is to see deeper targets and to characterize them better. The optimization of deep conductor detection is a complex exercise because there are so many aspects to consider. The main points are:

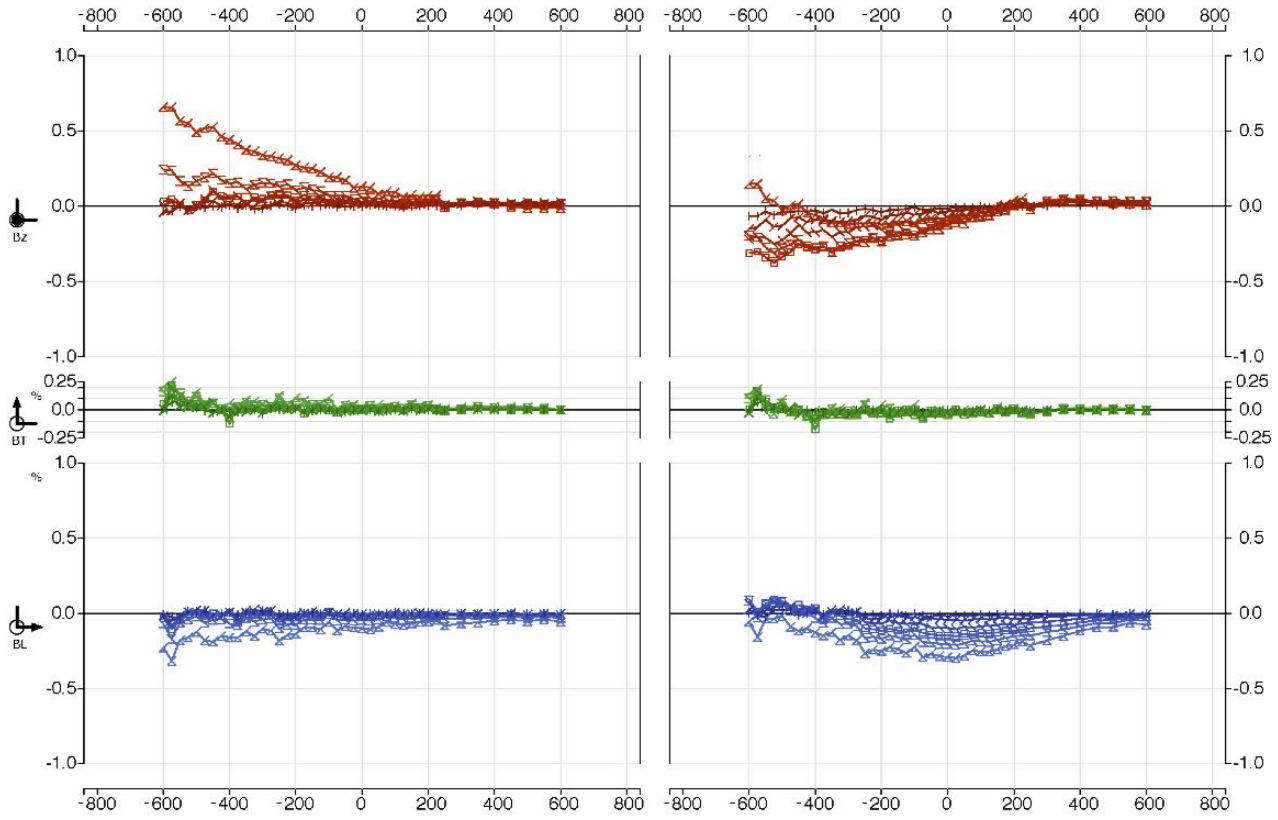

Figure 16: ***Left****: The last 6 channels (5.9 ms to 250 ms) field data profile measured at 2 Hz with the same size of loop as the model data located at the same relative location. There is only evidence of an overburden vanishing on late channels in data that shows a moderate noise level.* ***Right:*** *Adding in the model response we see that a clear target response would be clearly detectable in the conditions present in this survey area. The response could be modelled to roughly infer the target location and size.*

(1) The response of conductors gets smaller as their depth increases in relation to their size.
(2) The detection of conductors in the presence of a host response implies that only conductor with a sufficiently long lasting response can be detected.
(3) Broader responses of the same amplitude are more detectable because they are visible over many data stations and several survey lines.
(4) The decay time of a conductor response is not only dependent on the type of mineralization but to large extent on its size (thickness E and size W in the formula 1 above).
(5) Is the effective conductivity of a thicker conductor of the same mineralization greater because of the reduced effect of minor fractures and irregularities?
(6) At a given base frequency the decaying response of longer decay conductors decreases as the decay time increases.
(7) For UTEM this decrease is only by a factor of two but one has to consider that primary field reduced responses have greater geophysical artifacts due to magnetic susceptibility effects and geometrical errors.
(8) As well measuring at lower frequencies increases measurements errors unless longer survey time is allowed.
(9) Then there is the question of the loop size and survey geometry to use for the most effective search and to keep the host response to a tolerable level.

In UTEM development it has been assumed that a sensitivity as uniform as possible in decay time and in space is an effective approach. Another parallel line of research has been the development of modelling tools that can be used to look at realistic exploration scenarios.

Modelling an exploration scenario

As a simple example we look at the detectability of a lense shaped conductor at a particular depth. Let us take a 40m by 440m by 290m ellipsoid to represent a blind massive sulphide body of roughly 10 million tonnes at depth. **Figure 15** shows the response of such a target at 750m depth-to-top. For the UTEM 5 system the response of this target at 2 Hz would be considered of small but detectable amplitude. It is 0.5% relative to the primary field or 1.7 pT (0.19 pT/A) at channel 6 (5.9ms) but has decayed to 0.2% or less at channel 3 and later (>47 ms). Still the signal to

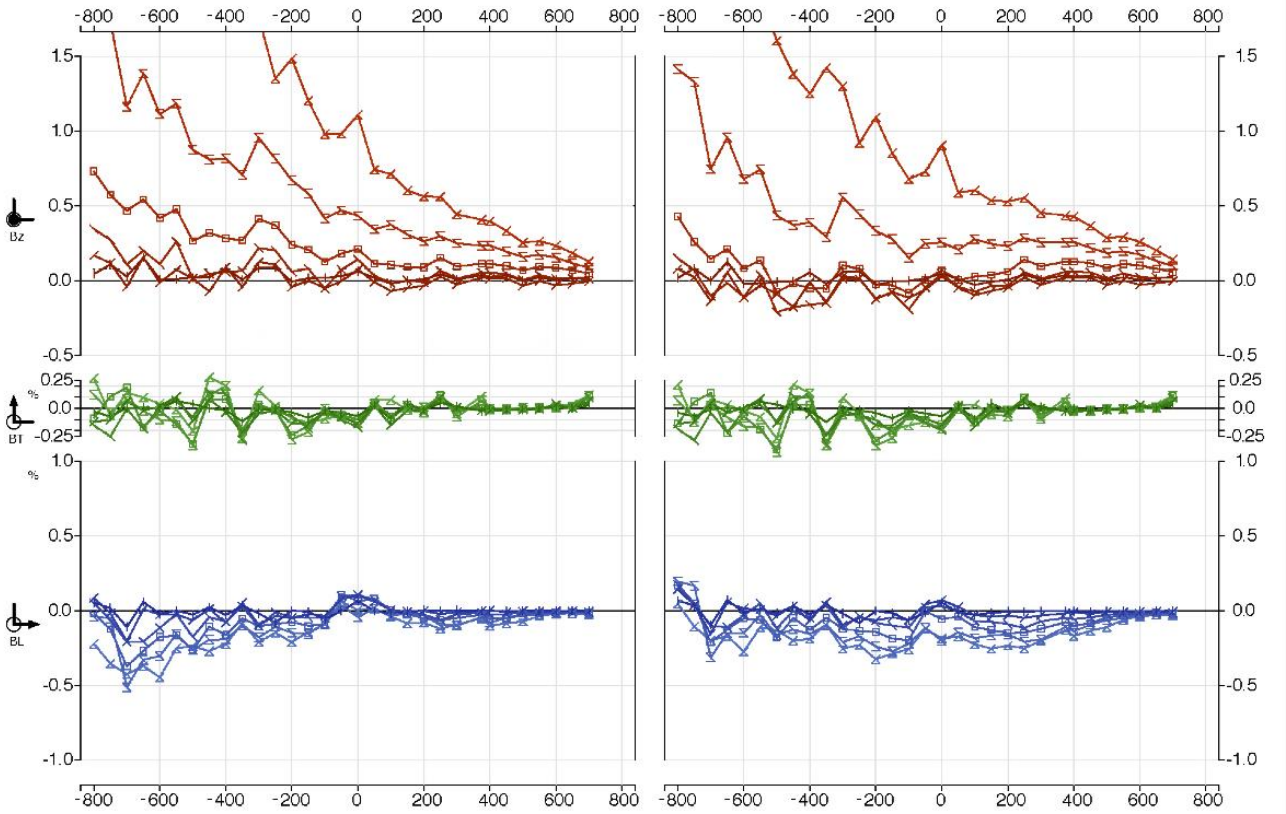

Figure 17: ***Left****: The last 6 channels (5.9 ms to 250 ms) field data profile measured at 2 Hz with the same size of loop as the model data located at the same relative location. There is evidence of a response due to a known long cultural conductor and also of noise due to power-line noise and road traffic.* ***Right:*** *Adding in the model response we see that the target conductor would be marginally detectable in the conditions present in this survey area. It is visible mainly on the B_L component because the anomaly is more compact and B_L has a lower noise level.*

noise in a quiet area would be more than 10:1 from channel 6 to channel 2 in late channel reduced data.

In **Figure 16** we see a comparison of a profile of the last channel reduced field data measured at 2 Hz in an area of moderate noise with the same survey geometry as the model wihout and with the MGEM model response added in.

(Adding EM responses is not strictly a valid exercise as any interactions between respective conductors in the two plots are not taken into account. In this case we assume it is roughly valid since the target conductor is far from the likely near surface source of the field data response and its long time decay is well decoupled from that overburden response.)

If we believe the result of this simple exercise, we can see that the target would be clearly detectable if located under this field traverse line and likely defined well enough to be immediately targeted with a borehole.

Figure 17 shows an example collected in an area affected by cultural noise and also a long cultural conductor some distance from the line with without and with the model conductor response. The late channel noise level is almost ten times greater than that of **Figure 16**. In this case the conductor would possibly be detected in a routine survey but with much less confidence. It would help if there were parallel traverse lines providing confirmation of the response. Before drilling this conductor it would be necessary to do detail surveying with longer stacks and perhaps schedule the survey at a time with less vehicular activity around the site.

What if the conductive target was 100 times more conductive such that there was practically no decay in the response? Then if we had still measured at 2 Hz a virtually un-decaying anomaly of 0.25% would have resulted which would not be detectable except with very accurate survey geometry and in an area without any magnetic anomalies. The only hope with such a target is that if an anomaly was at least suspected it may be possible in some cases to resolve such a small un-decaying anomaly with multiple transmitter loop coverage.

Multiple transmitter applications

UTEM 5 makes it possible to measure the responses of up to three transmitter loops at once. The use data from multiple transmitter loops can be useful in resolving anomalies of marginal amplitude including cases where a conductor is minimum coupled with one loop and other cases where there is possible interference form magnetic susceptibility anomalies.

To reduce the effect of a suspected magnetic susceptibility anomaly relative to the EM response of a steeply dipping targets, with multiple transmitter loops it is possible to use a linear combination of responses of multiple transmitter loops to vary the combined primary field direction at the suspected magnetic body centre so as to minimum couple the magnetic response. This process named simply “Combine” has also been used to determine the dip and strike direction of very deep targets.

CONCLUSIONS

The UTEM system has seen an order of magnitude improvement in accuracy and low frequency range over the last ten years to make it more effective in mineral exploration. In parallel to the hardware developments software developments not described in this paper have greatly contributed to the effectiveness of the UTEM system, notably web based data processing and modelling tools. Some results of the developments described have been applied since 2012 in the form of UTEM 5 surface surveys.

REFERENCES

Lamontagne, Y., Applications of wideband time-domain EM measurements in mineral exploration: Ph. D. thesis, Dept of Physics, Univ. of Toronto.

Lamontagne, Y., Deep exploration with EM in boreholes: Proceedings of Exploration 07, Fifth Decennial Conference on Mineral Exploration, paper 24, p. 401-415.

Macnae, J.C., Y. Lamontagne, and G.F. West, Noise processing techniques for time-domain EM systems: Geophysics v. 49, p. 934-948.

West G.F., J.C. Macnae, and Y. Lamontagne, A time-domain system measuring the step response of the ground: Geophysics v. 49, p. 1010-1026.